Electronic Supplementary Material 1:
Details on data acquisition, processing and modelling.

1) The study sites

ESM 1 Table 1: Topographic, environmental and floristic characteristics of the two study areas.

	French site (FR)	Swiss site (CH)
Location name	Roche Noire	Anzeindaz
Geographic coordinates	45°2.3' to 45°4.2'N 6°21.6' to 6°25.2'E	46°15' to 46°18'N, 7°07' to 7°11'E
Elevation range	1900 m to 3000 m	1650 m to 2150 m
Mean annual temperature	4.8°C	1.3 °C
Mean summer precipitation	180 mm	485 mm
Bed rock	Flysch	Calcareous
Number of inventoried plots	103	68

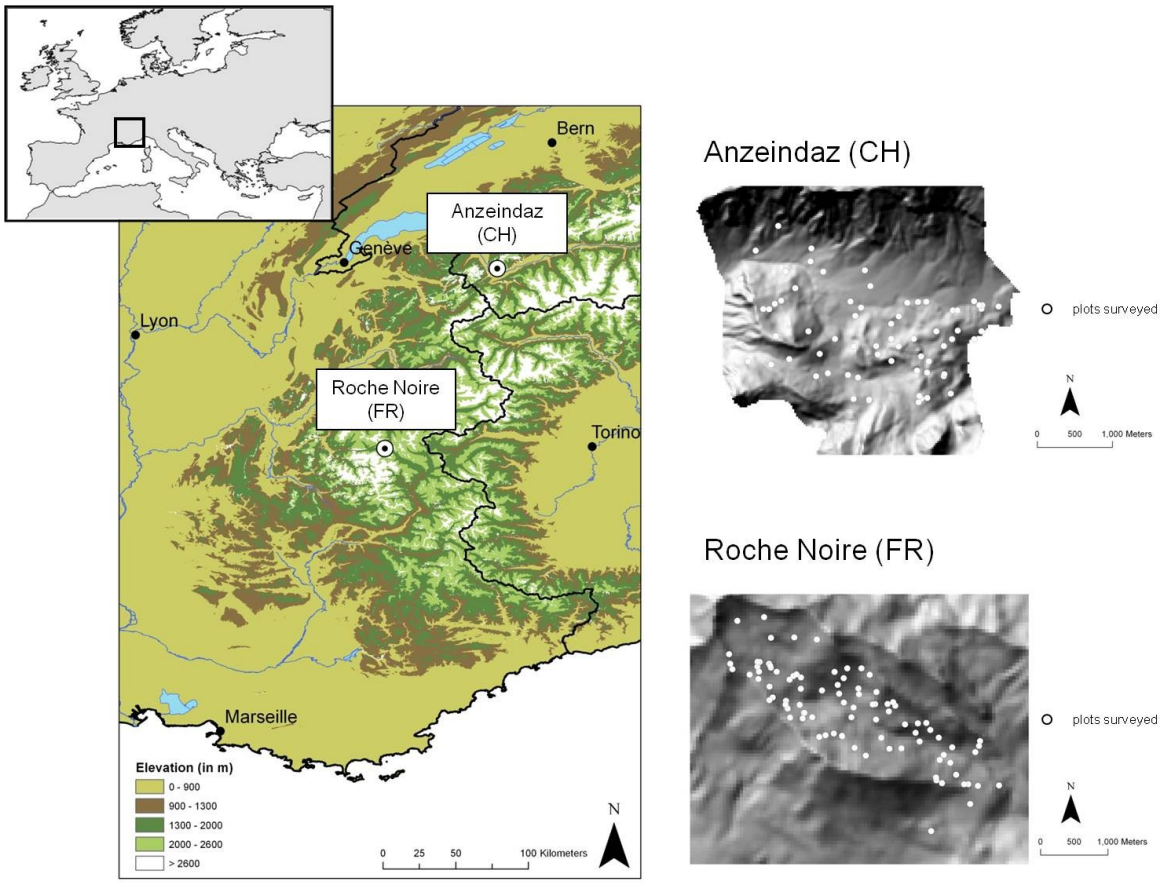

ESM 1 Fig. 1: Location of the two study areas. The minimum distance between vegetation plots is 21.91 m (mean of 1327.71 m) for FR and 12.67 m (mean of 1307.44 m) for CH.

2) Floristic data

Vegetation sampling was based on random stratified sampling designs to ensure covering equally well the different vegetation types of both FR and CH. Size of vegetation plots was chosen to approach exhaustive recording of the species. As vegetation structure differed between both sites, 2 m quadrat was chosen for CH and plots of 5 m in radius for FR. In addition, few plots of 2 m in radius were chosen in FR for sampling snowbelts. In such habitats species coexist at very fine scale so that reduced plot size still allow exhaustive sampling of the species of local vegetation patches. However, snowbelts are also characterised by fine scale vegetation changes in space. Thus, plots of 2 m in radius, compare to 5 m in radius, avoided bias in sampling associated vegetation type by edge effects.

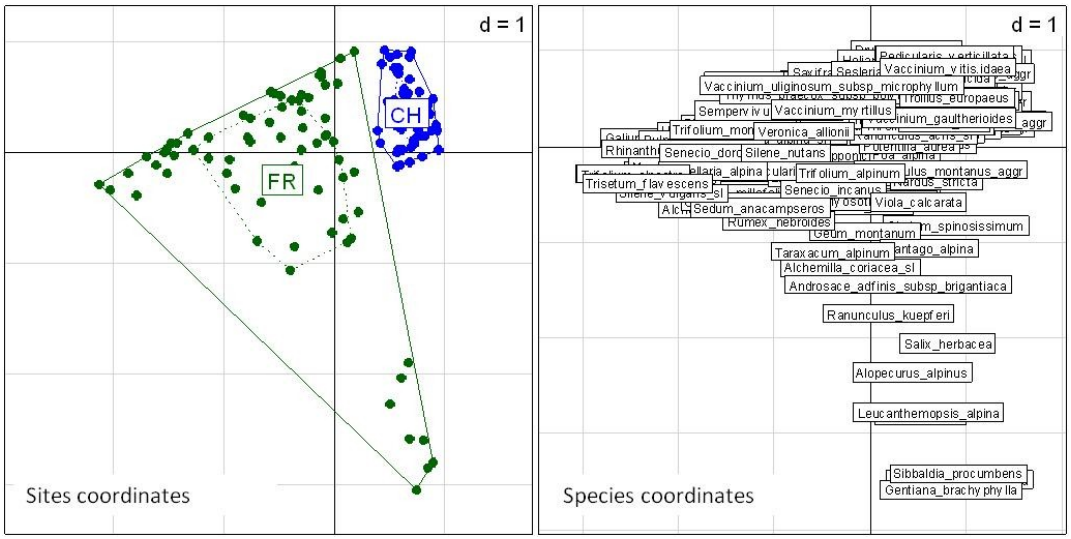

ESM1 Fig 2: Correspondence analysis of floristic data. Between site inertia ratio = 0.06 with *Pvalue*<0.001(Permutation test with 9999 permutations, alternative is greater).

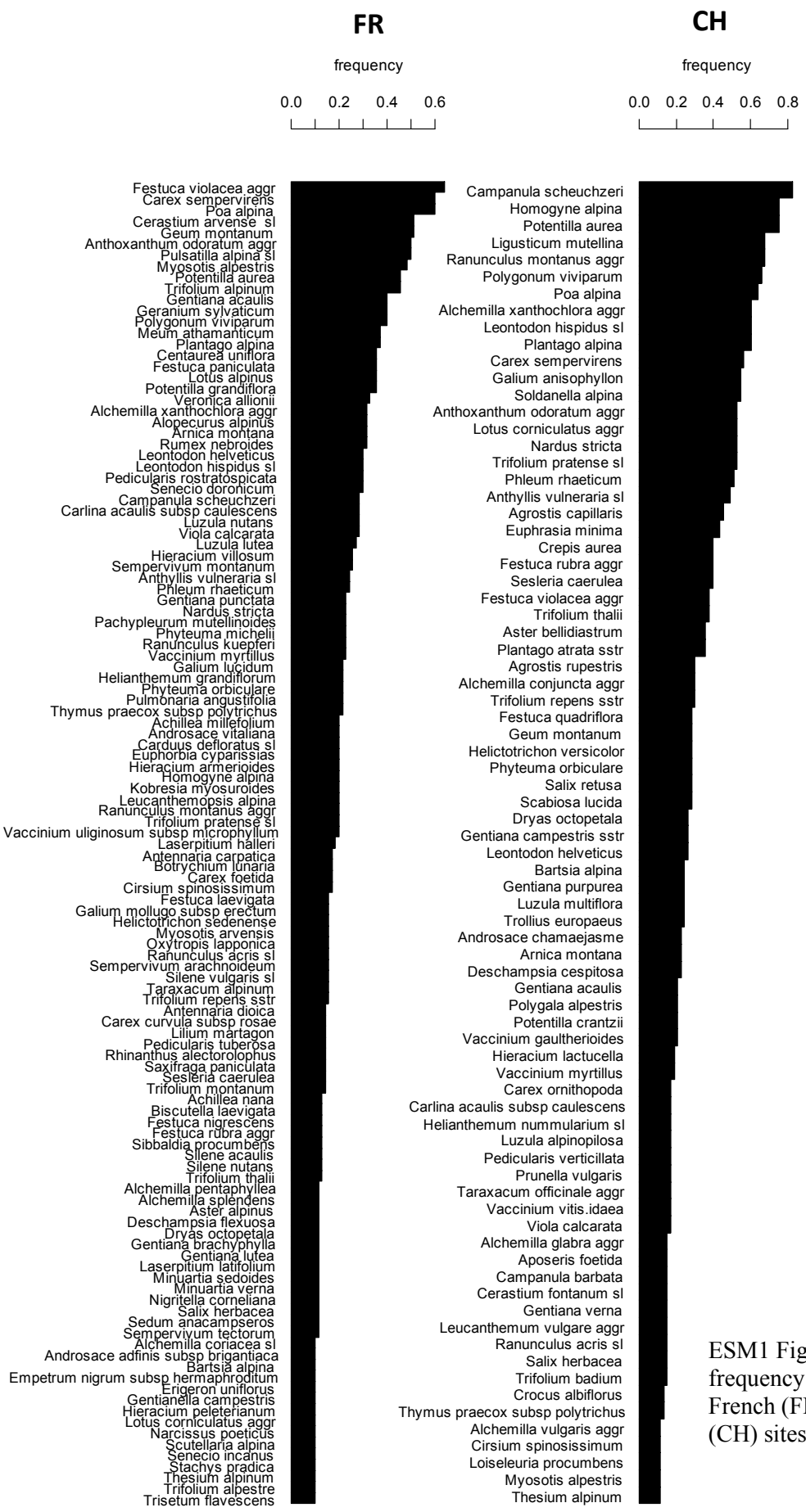

ESM1 Fig 3: Species rank-frequency curves for the French (FR) and Swiss (CH) sites.

3) Topographic predictors

We computed five predictors derived from digital elevation models at 50 m resolution for FR and 25 m resolution for CH, providing useful information on meso-scale habitat conditions in species distribution models [1]. Topographic predictors were: 1) elevation (in meters); 2) slope (in degrees); 3) aspect (in degrees from north); 4) Topographic Position Index (TPI), an integrated measure of topographic exposure (unitless) [2]; 5) Topographic Wetness Index (TWI), which quantifies topographic control on soil moisture (unitless), [3]. The last is calculated as follows TWI = ln(a / tan(b)) where a is the area of the upstream contribution (flow accumulation) and b is the slope in radians .

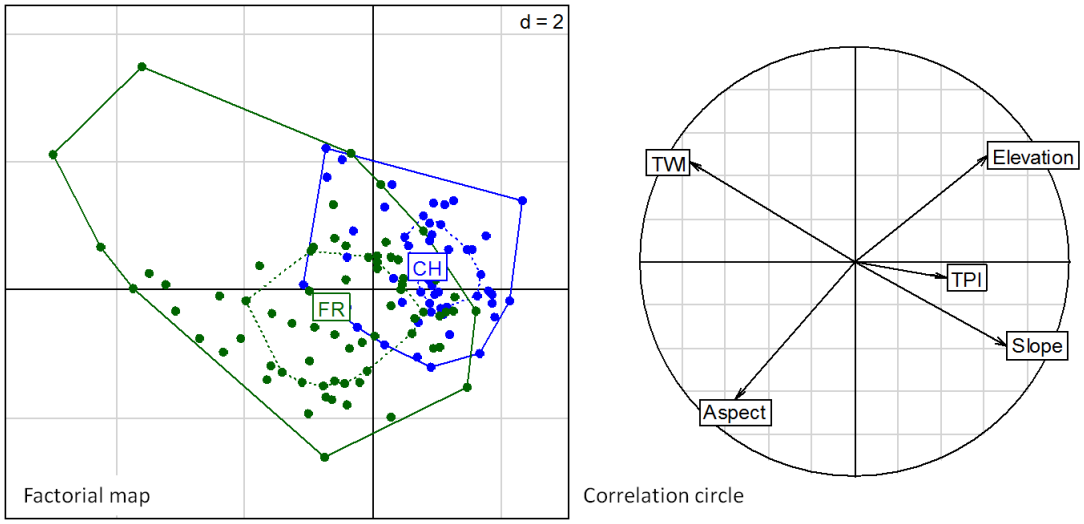

ESM1 Fig 4: Principal component analysis of the topographic predictors. Between site inertia ratio = 0.14 with *Pvalue*<0.001(Permutation test with 9999 permutations, alternative is greater). This result shows that topographical conditions of vegetation plots differ between the French (FR) and Swiss (CH) sites.

4) Remote sensing predictors

a. Airborne image acquisition and processing

The airborne imaging spectroscopy (AIS) data were acquired with an AISA Dual system (Specim, Ltd. Finland). Images of the French study site (FR) were collected on 23rd July 2008

and for the Swiss study site (CH) on 24th July 2008 under clear sky and sunny conditions. Images were acquired in a high spectral and spatial resolution mode, which resulted in a spectral image data cube with 359 narrow spectral bands between 400 and 2450 nm and the ground pixel size of 0.8 m.

The basic processing of AISA Dual images comprised of radiometric, geometric, and atmospheric correction. The radiometric correction that converted image digital numbers into radiance values [$W.m^{-2}.sr^{-1}.\mu m^{-1}$] was performed in the CaliGeo software (CaliGeo v.4.6.4 - AISA processing toolbox, Specim, 2007) using the factory delivered radiometric calibration coefficients. Images were geometrically corrected using the onboard navigation data from the Inertial Navigation System and a local digital elevation model (spatial resolution of 2.5 m for FR and 1 m for CH site). Images were further orthorectified into the Universal Transverse Mercator (UTM, Zone 32N) map projection. An accuracy of the geometric correction was evaluated by calculating an average root mean square error (RMSE) between distinct image displayed and ground measured control points. Assessment resulted into an average RMSE of about 2.04 m for the French site and about 1.25 m for the Swiss site. Atmospheric corrections were combined with vicarious radiometric calibrations in the ATCOR-4 software [4]. To eliminate random noise, spectra of the atmospherically corrected images were smoothed by a moving average filter with the window size of 7 bands. Accuracy of the atmospheric corrections was evaluated by comparing image surface reflectance with a set of ground measured reference spectra. An average reflectance RMSE between the image and the ground target spectra was equal to 2.1% for the French and 1.6% for the Swiss site. As the final step of the image processing we applied a fully constrained linear spectral unmixing algorithm [5] to identify pixels with high vegetation fraction. Only pixels with vegetation fraction higher than 75% were included into further analysis of species distribution modelling.

We paired the AISA image data with the georeferenced plots, where floristic species composition was investigated in-situ. Their geographical locations were superimposed over the AISA images and the reflectance function of each a research plot was averaged. Plots with high proportion of non-vegetated pixels (i.e. pixels with vegetation fraction lower than 75% due to the occurrence of stones or bare soil patches) were excluded. After this selection, we retained 70 plots at the French site and 53 plots at the Swiss site. Two types of remote sensing predictors were tested for the species distribution modelling: i) reflectance intensity of 75 noise-free bands and ii) four vegetation indices (summarized in Table 2).

b. Removal of spectral bands with low signal quality

Only 75 spectral bands out of 359 were included in the species distribution analysis. We removed bands with poor signal quality due to the low radiometric sensitivity at the edges of both sensor spectral ranges (401-444, 876-1140 and around 2450 nm), bands strongly influenced by atmospheric water vapor absorption (i.e., 1334-1485 and 1786-1968 nm) and adjacent bands of near infrared wavelengths between 752 and 771 nm, which are highly correlated and contain redundant spectral information.

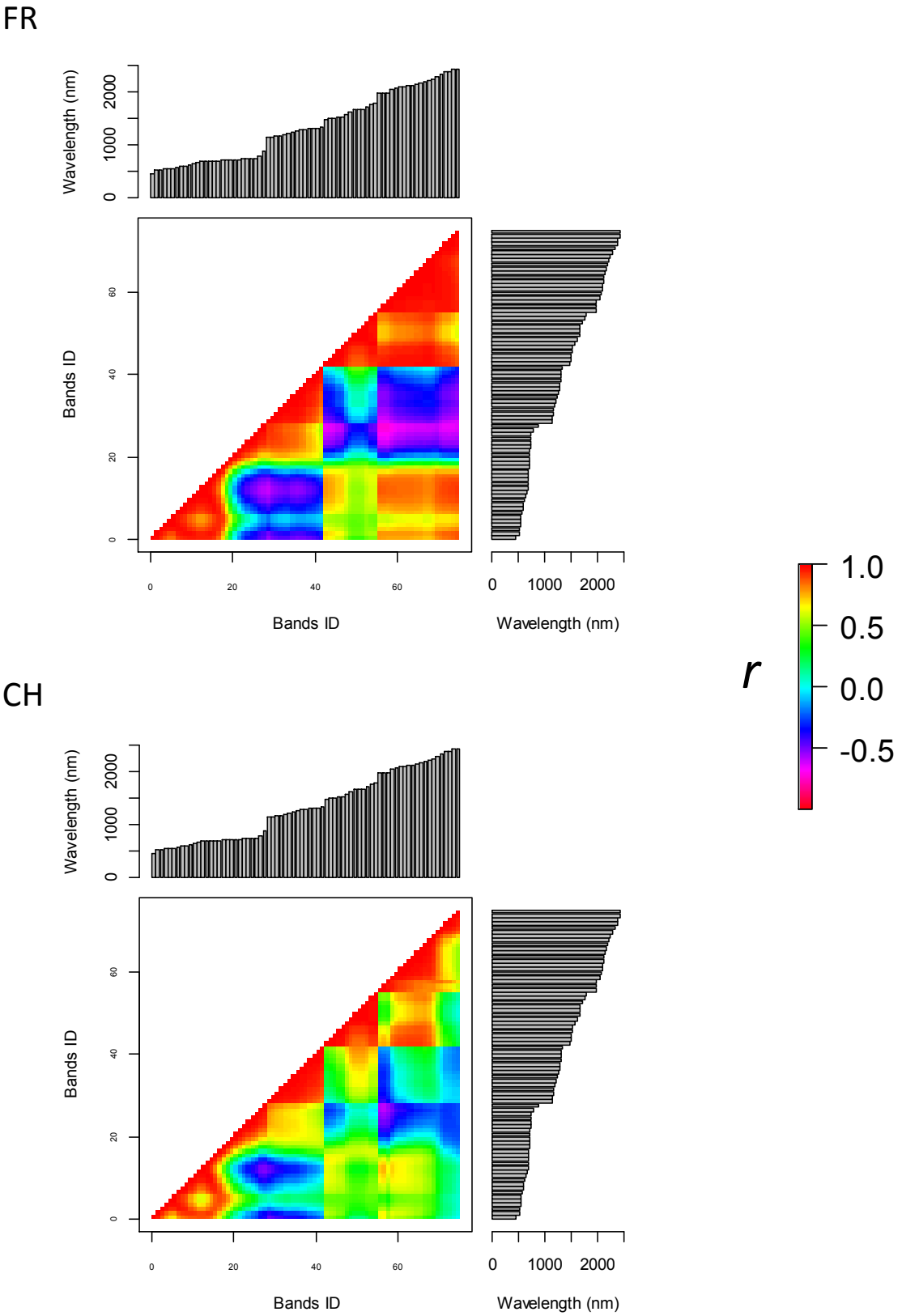

ESM1 Fig 5: Between reflectance bands correlation patterns for the French (FR) and Swiss (CH) sites. Although band selection (75 out of 359) led to the removal of highly correlated adjacent bands, many non-adjacent bands were strongly correlated. This justifies the use of unbiased conditional random forest in case of multicolinearity.

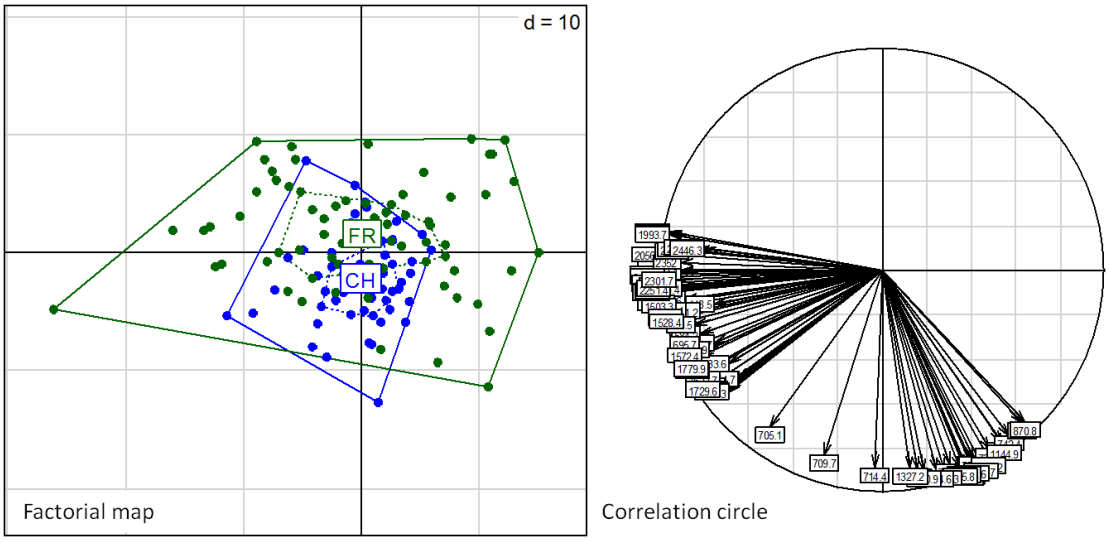

ESM1 Fig 6: Principal component analysis of the 75 reflectance bands. Between site inertia ratio = 0.06 with *Pvalue*<0.001(Permutation test with 9999 permutations, alternative is greater). This result shows that reflectance pattern of vegetation plots differed between the French (FR) and Swiss (CH) sites.

c. Calculation of vegetation indices and the between site PCA

Four vegetation optical indices, defined in Table 2, were selected as remote sensing indicators of the vegetation biochemical and biophysical properties. Two indices are highly sensitive to leaf chlorophyll content, but insensitive to the variations in amount of green biomass (TCARI/OSAVI and $ANCB_{650\text{-}720}$). MTVI2 index was chosen as an indicator of green leaf area index, while suppressing negative confounding influence of leaf chlorophyll content. Finally, SIWSI index is sensitive to plant water content. The variability of the selected optical indices is expected to be species composition specific in accordance with the species-specific changes of the related biochemical and biophysical characteristics. These four indices can thus potentially discriminate key properties of the species, justifying their use for species distribution modeling.

EMS 1 Table 2: Vegetation indices tested for species distribution modeling

Vegetation index	Equation		Reference
Transformed Chlorophyll Absorbtion Reflectance Index / Optimized Soil-Adjusted Vegetation Index (TCARI/OSAVI)	$\mathrm{TCARI} = 3[\mathrm{R}_{700} - \mathrm{R}_{670} - 0.2(\mathrm{R}_{700} - \mathrm{R}_{550})(\mathrm{R}_{700}/\mathrm{R}_{670})]$ $\mathrm{OSAVI} = \frac{1.16(R_{800} - R_{670})}{R_{700} + R_{670} + 0.16}$		Haboudane et al, (2002) [5]
Area under curve Normalized to the Continuum-removed Band depth ($ANCB_{650\text{-}720}$)	$\frac{\mathrm{AUC}_{650-720}}{\mathrm{CBD}_{670}}$	where $AUC_{650\text{-}720}$ is area under continuum removed reflectance between 650-720 nm and CBD_{670} is continuum removed band depth at 670 nm	Malenovský et al. (2013) [6]
Modified Triangular Vegetation Index (MTVI2)	$\frac{1.5[1.2(\mathrm{R}_{800} - \mathrm{R}_{550}) - 2.5(\mathrm{R}_{670} - \mathrm{R}_{550})]}{\sqrt{(2\mathrm{R}_{800} + 1)^2 - (6\mathrm{R}_{800} - 5\sqrt{\mathrm{R}_{570}}) - 0.5}}$		Haboudane et al. (2004) [7]
Shortwave Infrared Water Stress Index (SIWSI)	$\frac{\mathrm{R}_{858.5} - \mathrm{R}_{1640}}{\mathrm{R}_{858.5} + \mathrm{R}_{1640}}$		Cheng et al. (2006) [8]

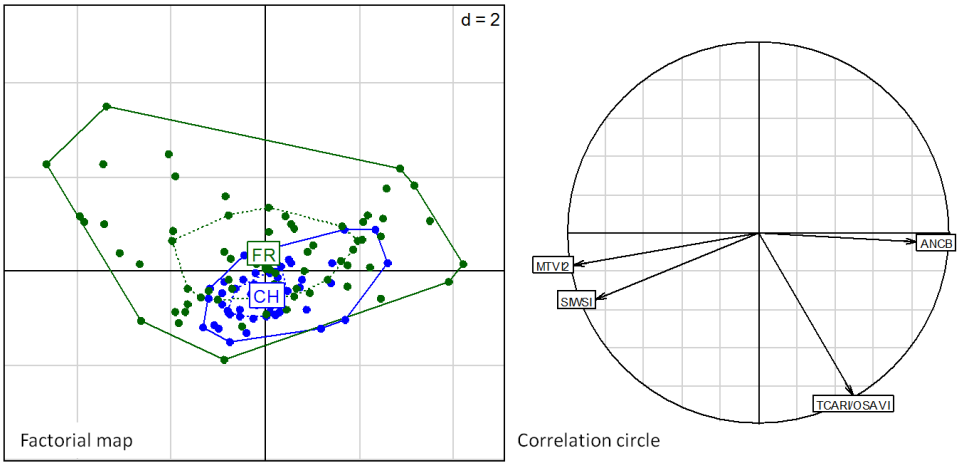

ESM1 Fig 7: Principal component analysis of the remote sensing predictors (vegetation indices. Between site inertia ratio = 0.05 with *Pvalue*=0.003 (Permutation test with 9999 permutations, alternative is greater). This result shows that reflectance indices of vegetation plots differed between the French (FR) and Swiss (CH) sites.

d. Correlation of AIS-data with topographic predictors

AIS and topographical data were weakly correlated (max absolute values for Pearson correlations amounted to 0.40-0.55 between elevation and bands in the range of 2000 and 2500 nm, while most of absolute values for Pearson correlation coefficients are between 0 and 0.3). Absence of strong correlation allows for mixing both types of data in species distribution models, as topographic- (indicating meso-scale habitat suitability of the species) and fine-scale AIS-data may represent complementary information.

5) Selection of spectral bands for building final species distribution models

Based on the analysis performed to quantify the importance of each of the 75 spectral bands, we built final species distribution models according to the following variable selection procedure:

1. Rank bands in decreasing order of importance
2. While not all bands have been considered, select the first ranked band (with the highest relative importance) and remove all bands showing correlation >0.7 with the previously selected band.

This procedure was performed with random forest (RF) using conditional inference trees as base learners and was implemented with the *party* library [9] for R [10]. Variable importance is measured as the mean decrease in accuracy of model predictions after permuting the predictor variables.

References

1. Pradervand, J.-N., Dubuis, A., Pellissier, L., Guisan, A. & Randin, C. 2013 Very high resolution environmental predictors in species distribution models: Moving beyond topography? *Prog. Phys. Geogr.* **38**, 79–96. (doi:10.1177/0309133313512667)

2. Zimmermann, N. E., Edwards, T. C., Moisen, G. G., Frescino, T. S. & Blackard, J. A. 2007 Remote sensing-based predictors improve distribution models of rare, early successional and broadleaf tree species in Utah. *J. Appl. Ecol.* **44**, 1057–1067. (doi:10.1111/j.1365-2664.2007.01348.x)

3. Beven, K. J. & Kirkby, M. J. 1979 A physically based, variable contributing area model of basin hydrology. *Bull. Int. Assoc. Sci. Hydrol.* **24**, 43–69.

4. Richter, R. & Schlapfer, D. 2002 Geo-atmospheric processing of airborne imaging spectrometry data. Part 2: Atmospheric/topographic correction. *Int. J. Remote Sens.* **23**, 2631–2649. (doi:10.1080/01431160110115834)

5. Haboudane, D., Miller, J. R., Tremblay, N., Zarco-Tejada, P. J. & Dextraze, L. 2002 Integrated narrow-band vegetation indices for prediction of crop chlorophyll content for application to precision agriculture. *Remote Sens. Environ.* **81**, 416–426. (doi:10.1016/S0034-4257(02)00018-4)

6. Malenovský, Z., Homolová, L., Zurita-Milla, R., Lukeš, P., Kaplan, V., Hanuš, J., Gastellu-Etchegorry, J.-P. & Schaepman, M. E. 2013 Retrieval of spruce leaf chlorophyll content from airborne image data using continuum removal and radiative transfer. *Remote Sens. Environ.* **131**, 85–102. (doi:10.1016/j.rse.2012.12.015)

7. Haboudane, D., Millera, J. R., Pattey, E., Zarco-Tejada, P. J. & Strachan, I. B. 2004 Hyperspectral vegetation indices and novel algorithms for predicting green LAI of crop canopies: Modeling and validation in the context of precision agriculture. *Remote Sens. Environ.* **90**, 337–352. (doi:10.1016/j.rse.2003.12.013)

8. Cheng, Y.-B., Zarco-Tejada, P. J., Riaño, D., Rueda, C. A. & Ustin, S. L. 2006 Estimating vegetation water content with hyperspectral data for different canopy scenarios: Relationships between AVIRIS and MODIS indexes. *Remote Sens. Environ.* **105**, 354–366. (doi:10.1016/j.rse.2006.07.005)

9. Strobl, C., Hothorn, T. & Zeileis, A. 2009 Party on! A New, Conditional Variable Importance Measure for Random Forests Available in the party Package. , 1–4.

10. R Core Team 2013 R: A Language and Environment for Statistical Computing.